J. Fluid Mech. (1986), *vol.* 162, *pp.* 261–282
Printed in Great Britain

Energetics and optimum motion of oscillating lifting surfaces of finite span

By ALI R. AHMADI† AND SHEILA E. WIDNALL
Massachusetts Institute of Technology, Cambridge, Massachusetts 02139

(Received 28 February 1985 and in revised form 24 June 1985)

The energetics of an unswept wing of finite span oscillating harmonically in combined pitch and heave in inviscid incompressible flow are determined in closed form. The calculations are based on a recently developed low-frequency unsteady lifting-line theory. The energetic calculations for the wing consist of sectional and total values of thrust, leading-edge suction force, power required to maintain the wing oscillations, and energy-loss rate due to vortex shedding in the wake, where the latter quantity is only defined for the entire wing. These results are used to analyse the optimum motion of a wing oscillating harmonically: optimum motion minimizes the power input for fixed average total thrust. The optimum solution is found to be unique (at least for low reduced frequencies), in contrast to the two-dimensional optimum, which is non-unique. Numerical results are presented for the energetics and optimum motion of an elliptic wing.

To understand better the structure of the known solution for the optimum motion of an oscillating two-dimensional airfoil, the solution is recast in terms of the normal modes of the energy-loss-rate matrix. It is found that one of the modes, termed here the 'invisible mode', plays a central role in the optimum solution and is responsible for its non-uniqueness. The three-dimensional optimum, which is unique, does not have an invisible mode.

1. Introduction

Very high efficiencies (compared with man-made vehicles) are observed in certain modes of animal propulsion in nature, such as bird flight and fish swimming. This is particularly true for high-aspect-ratio lunate-tail propulsion of many fast-moving fish, such as sharks and cetacean mammals, and the flapping flight of birds with high-aspect-ratio wings, such as gulls and albatross. Such wing and tail motions are typically associated with relatively high Reynolds numbers, where viscous effects are confined to a thin boundary layer at the surface and a thin trailing wake. Hence, the propulsive forces, which are generated primarily by the inertial forces, can be calculated from potential-flow theory using linearized unsteady-wing theory (for small-amplitude oscillations).

Prediction of the propulsive performance of an oscillating lifting surface, involves calculation of the energetic quantities: thrust, leading-edge suction force, power required to maintain the wing oscillations, and energy-loss rate due to vortex shedding in the wake. The hydrodynamic efficiency of the motion is defined as the ratio of the rate of work of average thrust to the average power required to maintain the motion. An interesting related problem is to determine the optimum shapes and

† Present address: Aerospace Engineering Department, California State Polytechnic University, Pomona, California 91768.

motions that give rise to the highest attainable hydrodynamic efficiency. This problem is concerned with those shapes and motions of the lifting surface that produce a prescribed level of thrust at minimum energy cost in maintaining the motion.

In two dimensions, the energetic quantities for a harmonically oscillating airfoil have been calculated by von Kármán & Burgers (1935), Garrick (1936) and Lighthill (1970), for small-amplitude motion. Calculations for a flexible airfoil have been carried out by Wu (1961) and Siekmann (1962, 1963) for constant forward speed, and by Wu (1971*a*) for general transverse oscillations and variable forward speed. Chopra (1976) considered the cases of irregular and regular heaving motion of large amplitude with small-amplitude pitching motion about the local path and assumed a rigid wake.

The only analysis of the optimum problem is the two-dimensional one of Wu (1971*b*), who determined (i) the optimum motion of an airfoil oscillating harmonically in pitch and heave and (ii) the optimum shapes and motions of a harmonically oscillating flexible airfoil (infinite degrees of freedom). For the former he found that the solution is not unique, with the amplitude of heave remaining arbitrary. In the present work, Wu's optimum solution for this case is recast in terms of the normal modes of the energy-loss-rate matrix to shed light on the structure of the optimum. It is found that the optimum consists primarily of one of the modes, termed here the 'invisible mode', which is also responsible for the non-uniqueness of the solution. For the case of the flexible airfoil, Wu finds that the solution can be determined to a certain extent, but the exact shapes and motions cannot always be uniquely determined.

These studies overestimate the thrust and efficiency, since they do not account for finite-span effects. To account for finite-span effects, Betteridge & Archer (1974) and Archer, Sapuppo & Betteridge (1979) used quasi-steady lifting-line theory, which underestimates the unsteady effects. Bennet (1970) based his calculations on the approximate unsteady lifting-surface theory of Reissner (1947). Chopra (1974) used superposition of sinusoidal lifting ribbons of infinite span for a rectangular wing in combined pitch and heave. His analysis is limited to the rectangular planform.

Others have based their calculations on numerical unsteady lifting-surface theory. Chopra & Kambe (1977) employed the kernel-function method for a family of wing planforms, most of which are swept back. Lan (1979) used the 'quasi-vortex-lattice' method for rigid wings of rectangular and arrow planform, including a tandem wing configuration. Agreement between the two theories is not as good as expected and warrants further work on the lifting-surface approach to this problem. In three dimensions, there has been no analysis of the problem of optimum shapes and motions. This is primarily because of a lack of an adequate three-dimensional unsteady aerodynamic theory with closed-form results. Lighthill (1970) suggested the use of unsteady lifting-line theory for the study of the propulsive performance of high-aspect-ratio lunate tails (also applicable to high-aspect-ratio bird wings).

In the present work, we use a recently developed linearized, low-frequency, unsteady lifting-line theory (Ahmadi 1980; Ahmadi & Widnall 1982, 1985) to calculate the (sectional and total) energetic quantities and optimum motion of an oscillating wing of finite span. This approach has several advantages: (i) all of the results are obtained in closed form, suited for optimization studies; (ii) compared with lifting-surface theory, computation time is reduced substantially; and (iii) in the present acceleration-potential formulation of the problem, the leading-edge suction force is obtained exactly (linearized and to leading order in inverse aspect ratio). The

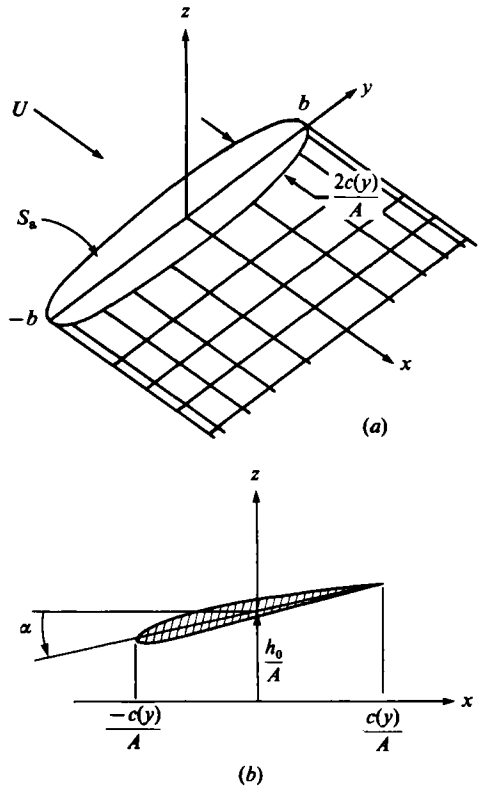

FIGURE 1. (*a*) Schematic of the wing in unsteady motion; (*b*) positive direction of pitch and heave for wing sections.

latter is in contrast with numerical lifting-surface calculations in steady and unsteady flows, where the suction force is obtained approximately (see Wagner 1969; Lan 1979).

2. Energetics of oscillating wings

In this section, we calculate the sectional and total energetic quantities – namely thrust, leading-edge suction force, power required to maintain the wing oscillations, and energy-loss rate due to vortex shedding in the wake – for an unswept wing of finite span oscillating harmonically in combined pitch and heave. The calculations are carried out using a recently developed low-frequency unsteady lifting-line theory (see Ahmadi 1980; Ahmadi & Widnall 1982, 1985), whose principal results are summarized in the Appendix. For harmonic motion, only the time average of the energetic quantities enter into the results. All calculations are carried out to leading order in inverse aspect ratio, with errors of $O(A^{-2})$.

We consider a thin, unswept wing of large aspect ratio executing small-amplitude, harmonic pitch and heave oscillations in a uniform stream of inviscid incompressible fluid with velocity U directed along the x-axis. The wing planform is described by $x = \pm c(y)/A$, $|y| \leqslant b$, $z = 0$ in a Cartesian coordinate system (x, y, z) attached to the mean position of the wing (see figure 1*a*). A is the wing aspect ratio defined as

$A = (2b)^2/S_a$, where b is the semi-span and S_a is the wing planform area. $c(y)/A$ is the semi-chord. Both b and $c(y)$ are $O(1)$. The transverse displacements of the wing are described by a heaving motion of amplitude h_0/A and a pitching motion about the mid-chord of amplitude α. α is complex to allow for arbitrary phase difference between pitch and heave.

$$z = h(x,t) = \left[\frac{h_0}{A} + \alpha x\right] e^{j\omega t}$$
$$= [\tfrac{1}{2}(c_0/A)\,\xi_0 + (\xi_1 + j\xi_2)\,x]\, e^{j\omega t} \quad \left(|x| \leqslant \frac{c(y)}{A},\ |y| \leqslant b\right), \tag{1}$$

where ξ_0, ξ_1, and ξ_2 are the non-dimensional heave/pitch amplitudes; c_0/A is the root semi-chord; j is the temporal complex unit; ω is the radian frequency of oscillation; and t is time. It is assumed that $\omega c(y)/U = O(1)$. The heaving motion is positive in the z-direction and the pitching motion is positive nose down (see figure 1*b*).

2.1. *Leading-edge suction force*

Thrust consists of the leading-edge suction force and a contribution from the normal force at the wing. First we calculate the suction force, which arises from the pressure singularity at the leading edge. In three dimensions, the suction force has been calculated numerically using unsteady lifting-surface theory (see e.g. Lan 1979). In the present work, we use unsteady lifting-line theory to calculate the suction force analytically.

According to lifting-line theory (see Appendix), three-dimensional effects arise at each wing section from induced downwash, shown to be a convecting sinusoidal gust, whose amplitude and phase vary with spanwise location. Interaction of this gust with wing sections modifies the local two-dimensional pressure field by an amount equal to the pressure field of the interaction of a convecting sinusoidal gust with an airfoil, i.e. the Sears Problem (Sears 1941). This changes the strength of the leading-edge singularity and hence the leading-edge suction force.

Formally, we calculate the suction force by applying Blasius' theorem to a small circle surrounding the leading edge in the cross-sectional plane of the wing. Ahmadi (1980) has shown that, in the neighbourhood of the leading edge, the complex velocity in the aforementioned plane behaves like

$$\tilde{g}(\zeta, y) = \tilde{u}(\boldsymbol{x}) - i\tilde{w}(\boldsymbol{x})$$
$$\sim \tfrac{1}{\sqrt{2}}[\tilde{a}_0(y) + 2S(k)\,\tilde{W}_g(y)]\left[\frac{c(y)/A}{\zeta + c(y)/A}\right]^{\frac{1}{2}} + O(1) \quad \left(\zeta \to \frac{-c(y)}{A}\right), \tag{2}$$

where u and w are, respectively, the x- and y-components of velocity; $\boldsymbol{x}$ is the position vector (x, y, z); $S(k)$ is the Sears function (see Appendix); $\tilde{W}_g(y)$ is the complex amplitude of unsteady induced downwash W_I (see Appendix); $\zeta = x + iy$; i is the spatial complex unit ($ij \neq -1$); $k = (\omega/U)\,c(y)/A$ is reduced frequency based on local semi-chord; and $\tilde{}$ denotes the complex amplitude of harmonic quantities. $\tilde{a}_0(y)$ is given by

$$\tilde{a}_0(y) = \tilde{b}_1(y) - [\tilde{b}_0(y) + \tilde{b}_1(y)]\,C(k), \tag{3}$$

where $C(k)$ is Theodorsen's function (see Appendix) and

$$\tilde{b}_n(y) = \frac{2}{\pi}\int_0^\pi \tilde{W}_0(x,y)\cos n\theta\, d\theta, \quad n = 0, 1, 2, \ldots \quad \left(x = \frac{c(y)}{A}\cos\theta\right) \tag{4}$$

are the coefficients of the chordwise Fourier cosine series for downwash at the wing

$$W_0 = \left(\frac{\partial}{\partial t} + U\frac{\partial}{\partial x}\right)h$$

$$= \tfrac{1}{2}b_0 + \sum_{n=1}^{\infty} b_n \cos n\theta.$$

Substituting (2) in Blasius' formula, integrating and averaging over time, we obtain the average suction force per unit length of the leading edge, which points along the outward normal to the edge and is taken positive in that direction:

$$\bar{T}_s(y) = \frac{\pi}{4}\rho\frac{c}{A}\mathrm{RP_j}\left[|\tilde{a}_0(y)|^2 + 4S^*(k)\,\tilde{a}_0(y)\,\tilde{W}_g^*(y)\right], \tag{5}$$

where ρ is fluid density, $\bar{\ }$ denotes time average, and $\mathrm{RP_j}$ and $(\ )^*$ respectively denote the real part and the complex conjugate of a complex quantity with respect to j. Since all of the energetic quantities in the present work are calculated to $O(A^{-1})$, in the derivation of (5) we have neglected a higher-order term of order $|W_I|^2 \sim O(A^{-2})$. Numerically, $\bar{T}_s(y)$ is also equal to the streamwise component of the average suction force per unit span. Hence, average total leading-edge suction for the wing is

$$\bar{\mathscr{T}}_s = \int_{-b}^{b} \bar{T}_s(y)\,dy.$$

We define the non-dimensional coefficients for average sectional and total suction force as

$$C_{T_s}(y^*) = \bar{T}_s(y)\Big/\left[\tfrac{1}{4}\pi\rho U^2\left(\frac{c_0}{A}\right)\right], \tag{6}$$

$$C_{\mathscr{T}_s} = \bar{\mathscr{T}}_s/[\tfrac{1}{4}\pi\rho U^2(\tfrac{1}{2}S_a)], \tag{7}$$

where $y^* = y/b$ is the non-dimensional spanwise coordinate.

2.2. *Thrust from the normal force*

The average value of the horizontal component of the normal force at the wing per unit span is given by

$$\bar{T}_p(y) = \int_{-c(y)/A}^{c(y)/A} \overline{\Delta p(x,y,t)\frac{\partial h}{\partial x}(x,y,t)}\,dx, \tag{8}$$

where $\Delta p = p(x,y,0-) - p(x,y,0+)$ is the pressure jump across the wing. For a wing in combined pitch and heave, (8) reduces to

$$\bar{T}_p(y) = \tfrac{1}{2}\mathrm{RP_j}\left[\alpha^*\tilde{l}(y)\right], \tag{9}$$

where $\tilde{l}(y)$ is the unsteady lift per unit span (see Appendix). We define the non-dimensional coefficients for average sectional and total thrust as

$$C_T(y^*) = \bar{T}(y)\Big/\left[\tfrac{1}{4}\pi\rho U^2\left(\frac{c_0}{A}\right)\right], \tag{10}$$

$$C_{\mathscr{T}} = \bar{\mathscr{T}}\Big/\left[\tfrac{1}{4}\pi\rho U^2(\tfrac{1}{2}S_a)\right], \tag{11}$$

where $\bar{T}(y) = \bar{T}_s(y) + \bar{T}_p(y)$ is the average thrust per unit span and $\bar{\mathscr{T}}$ is the average total thrust for the wing.

2.3. *Required power*

The average power required to maintain the wing oscillations per unit span is given by

$$\bar{P}(y) = -\int_{-c(y)/A}^{c(y)/A} \overline{\Delta p(x,y,t)\frac{\partial h}{\partial t}(x,y,t)}\,\mathrm{d}x. \tag{12}$$

For a wing in combined pitch and heave, this reduces to

$$\bar{P}(y) = \tfrac{1}{2}\mathrm{RP_j}\left\{\mathrm{j}\omega\frac{h_0}{A}\tilde{l}(y) - \mathrm{j}\omega\alpha^*\tilde{m}(y)\right\}, \tag{13}$$

where $\tilde{m}(y)$ is the unsteady moment about mid-chord per unit span taken positive nose up (see Appendix). We define the non-dimensional coefficients for average sectional and total power required as

$$C_P(y^*) = \bar{P}(y)\Big/\left[\tfrac{1}{4}\pi\rho U^3\left(\frac{c_0}{A}\right)\right], \tag{14}$$

$$C_{\mathscr{P}} = \bar{\mathscr{P}}/[\tfrac{1}{4}\pi\rho U^3(\tfrac{1}{2}S_a)], \tag{15}$$

where $\bar{\mathscr{P}}$ is the total average required for the wing.

2.4. *Energy-loss rate*

For a wing of finite span, energy-loss rate due to vortex shedding in the wake is defined only for the entire wing (no sectional value). The average total energy loss rate for the wing $\bar{\mathscr{E}}$ is obtained from the principle of conservation of mechanical energy:

$$\bar{\mathscr{E}} = \bar{\mathscr{P}} - U\bar{\mathscr{T}}. \tag{16}$$

We define a non-dimensional coefficient for $\bar{\mathscr{E}}$ as

$$C_{\mathscr{E}} = \bar{\mathscr{E}}/[\tfrac{1}{4}\pi\rho U^3(\tfrac{1}{2}S_a)]. \tag{17}$$

The hydrodynamic efficiency for the motion is defined as

$$\eta = C_{\mathscr{T}}/C_{\mathscr{P}} = 1 - C_{\mathscr{E}}/C_{\mathscr{P}}. \tag{18}$$

2.5. *Numerical examples*

Next, we present numerical examples for the above three-dimensional calculations of the energetic quantities for an oscillating wing. The examples demonstrate the influence of finite span on the energetic quantities and hydrodynamic efficiency for an oscillating elliptic wing. In each case, the corresponding strip-theory result (ST) is also shown for comparison. The energetic quantities for the heaving and the pitching wings are, respectively, normalized by ξ_0^2 and ξ_1^2 (see (1)). Numerical schemes for the calculation of finite-span effects are given in Ahmadi (1980).

Figure 2 shows the spanwise distribution of average required power for an elliptic wing ($A = 8$) in pitch for $k_0 = 0$, 0.1, and 0.3, where $k_0 = (\omega/U)\,c_0/A$ is the reduced frequency based on root semi-chord. The three-dimensional results are denoted by ULLT (unsteady lifting-line theory). Because of the influence of induced downwash, which reduces the amplitude of unsteady section lift and moment, the three-dimensional theory predicts less power required for maintaining the motion than does the strip theory. It is also seen that the required power grows with increasing reduced frequency k_0, as expected.

Figure 3 shows the spanwise distribution of the average leading-edge suction force

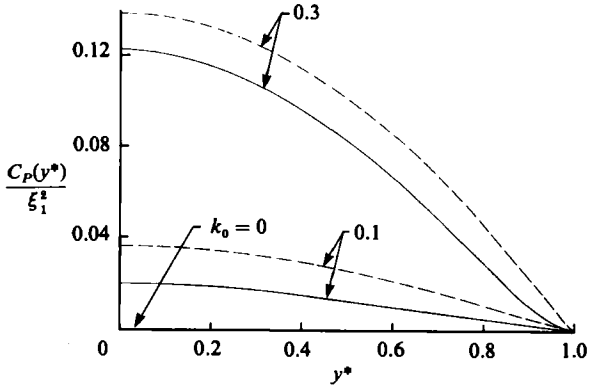

FIGURE 2. Spanwise distribution of required power for an elliptic wing in pitch, $A = 8$; ---, ST; ——, ULLT.

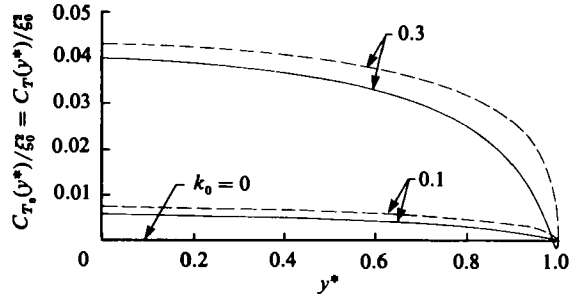

FIGURE 3. Spanwise distribution of leading-edge suction force and thrust for an elliptic wing in heave, $A = 8$; ---, ST; ——, ULLT.

for an elliptic wing ($A = 8$) in heave. Finite-span effects also reduce the suction force because induced downwash generally opposes the flow around the leading edge, and thus reduces the strength of the leading-edge singularity. The small region of negative suction force near the tip for $k_0 = 0.3$ in figure 3 is a result of neglecting a higher-order term of order $|W_I|^2 \sim O(A^{-2})$ in deriving the suction force, (5). Retaining this higher-order term will resolve the problem, since the amplitude of unsteady induced downwash $|W_I|$ can become quite large near the tip, especially at higher reduced frequencies k_0 (see figure 5 of Ahmadi & Widnall 1985). However, the accuracy of the results, $O(A^{-2})$, would be inconsistent with that of the other energetic quantities which are calculated to $O(A^{-1})$. Furthermore, since the suction force tends to zero at the tip and since the region of negative values is very small (about 1 % of semi-span at $k_0 = 0.3$), the effect of this on the total thrust is negligible.

Since for a heaving wing all of the thrust is contributed by the suction force, figure 3 also represents the spanwise distribution of average thrust for an elliptic wing in heave. Figure 4 shows the spanwise distribution of average thrust for a pitching wing. However, in the range $k_0 = 0$ to 0.3, the pitching wing produces negative thrust (i.e. drag), which is consistent with the known two-dimensional result. In the steady-flow limit, we obtain one half the steady induced drag. This factor of one half arises from time averaging, which is not meaningful in steady flow. Furthermore, because of the additional drag associated with the trailing vorticity, the three-dimensional unsteady drag is larger than that predicted by the strip theory. As

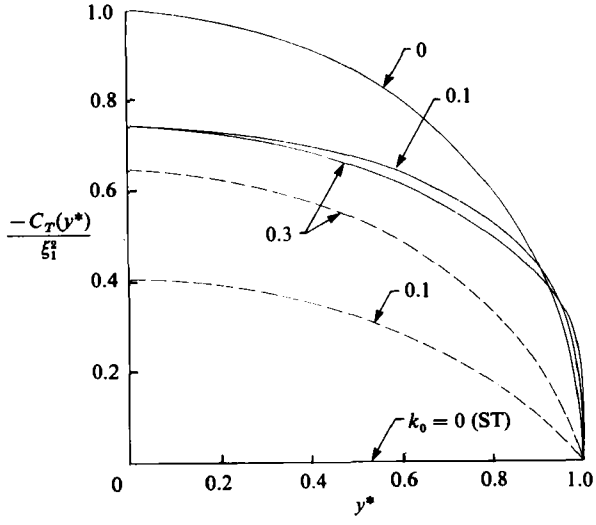

FIGURE 4. Spanwise distribution of section thrust (drag) for an elliptic wing in pitch, $A = 8$; ---, ST; ——, ULLT.

expected, all of the three-dimensional results approach their strip-theory counterparts with increasing reduced frequency k_0.

The next example shows the overall propulsive performance of an elliptic wing in combined pitch and heave. It is convenient to present these results in terms of Lighthill's (1970) description of wing displacements, namely

$$h(x,y,t) = [h_L - j\alpha_L(x-b_L)]e^{j\omega t} \quad (|x| \leqslant c(y)/A), |y| \leqslant b), \tag{19}$$

where h_L and α_L are real with respect to j and denote, respectively, the amplitudes of heave and pitch. The phase difference between the two modes of oscillation is fixed at 90°, but the position of the axis of pitch, $x = b_L$, $z = 0$, is variable. Lighthill's description is completely equivalent to the present one (see (1)) with the interrelations

$$\frac{h_L}{c_0/A} = -\tfrac{1}{2}\xi_0 \sin\alpha_P, \quad \alpha_L = (\xi_1^2+\xi_2^2)^{\frac{1}{2}} = \xi_0 Z_P, \quad \frac{b_L}{c_0/A} = \frac{-\frac{1}{2}\cos\alpha_P}{Z_P}, \tag{20}$$

where Z_P and α_P are, respectively, the amplitude ratio and the phase advance of pitch with respect to heave in the present notation:

$$Z_P = \frac{(\xi_1^2+\xi_2^2)^{\frac{1}{2}}}{\xi_0}, \quad \alpha_P = \tan^{-1}\left(\frac{\xi_2}{\xi_1}\right). \tag{21}$$

Furthermore, Lighthill's 'proportional feathering parameter' $\Theta_L = U\alpha_L/(\omega h_L)$, which is a measure of the deviation of the wing slope from the tangent to the path traversed in space by the pitch axis, is given by

$$\Theta_L = -2Z_P \operatorname{cosec}\frac{\alpha_P}{k_0}. \tag{22}$$

We use the above relations to express the results of the present calculations in terms of Lighthill's parameters.

Figure 5 shows the thrust coefficient $C_{\mathscr{T}}$ and the hydrodynamic efficiency η for an elliptic wing ($A = 16$) in combined pitch and heave in terms of Lighthill's parameters. The axis of pitch is at $\frac{3}{4}$ of root chord and a range of values of the feathering parameter

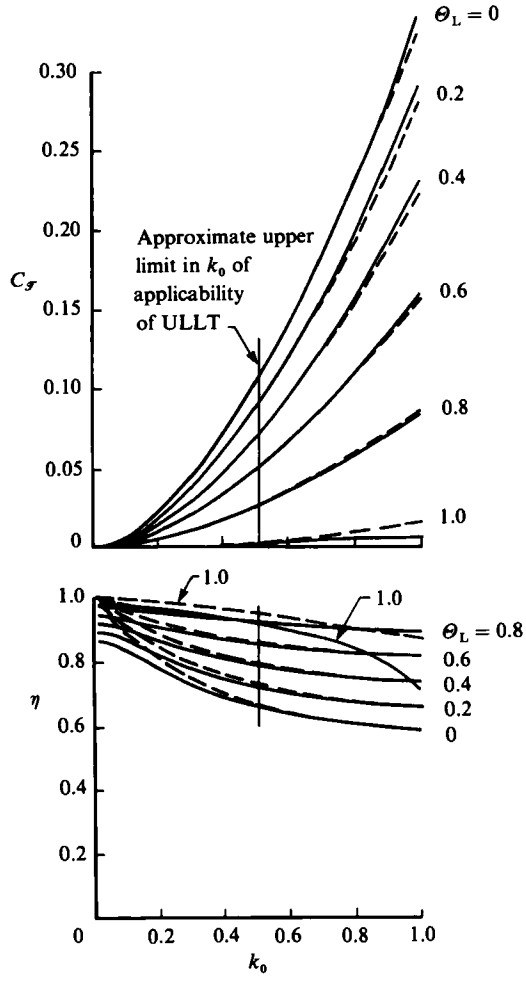

FIGURE 5. Thrust coefficient and hydrodynamic efficiency for an elliptic wing of $A = 16$ for several values of feathering parameter with axis of pitch located at $\frac{3}{4}$ of centre section chord; ---, ST; ——, ULLT.

Θ_L are considered. Also shown are the corresponding strip-theory results,† which closely resemble the two-dimensional results of Lighthill (1970), with η tending to 100% as $k_0 \to 0$ for all Θ_L. We note that, as $k_0 \to 0$, all configurations with $\Theta_L \neq 0$ tend to pure heaving motion as can be seen from the alternative form of Θ_L,

$$\Theta_L = \frac{\alpha_L}{k_0 h_L/(c_0/A)}.$$

Figure 5 shows that finite-span effects reduce η below the strip-theory values and η no longer approaches 100% in the steady limit, owing to the presence of trailing vorticity. The approximate range of applicability of the lifting-line theory for $A = 16$ is indicated in the figure (see figure 18 of Ahmadi & Widnall 1982).

The rest of this paper is devoted to the analysis of the optimum-motion problem.

† Non-dimensional coefficients for the strip theory are independent of aspect ratio.

3. Optimum motion of an oscillating airfoil

The general problem of determining the optimum shapes and motions of an oscillating lifting surface of fixed planform may be stated as follows: from within a prescribed class of shape functions $z = h(x, y, t)$, find the one that minimizes the power input for fixed average thrust.

Before considering the three-dimensional optimum, we first recast the known two-dimensional optimum for an airfoil in combined pitch and heave (Wu 1971*b*) in terms of the normal modes of the average-energy-loss-rate matrix. This sheds light on the structure of the two-dimensional optimum and is also helpful in understanding the three-dimensional optimum. The airfoil motion is described by:

$$z = h(x,t) = [\tfrac{1}{2}c\xi_0 + (\xi_1 + \mathrm{j}\xi_2)\,x]\,\mathrm{e}^{\mathrm{j}\omega t} \quad (|x| \leqslant c). \tag{23}$$

The average value of the energetic quantities, i.e. energy-loss rate, power required, thrust and leading-edge suction force, are, respectively, denoted by $\bar{E}$, $\bar{P}$, $\bar{T}$, and $\bar{T}_s$, or in non-dimensional form by

$$C_E = \bar{E}/[\tfrac{1}{4}\pi\rho U^3 c], \tag{24}$$

$$C_P = \bar{P}/[\tfrac{1}{4}\pi\rho U^3 c], \tag{25}$$

$$C_T = \bar{T}/[\tfrac{1}{4}\pi\rho U^2 c], \tag{26}$$

$$C_{T_s} = \bar{T}_s/[\tfrac{1}{4}\pi\rho U^2 c]. \tag{27}$$

In matrix notation, the corresponding quadratic forms are given by

$$C_E = \boldsymbol{\xi}^{\mathrm{T}}\boldsymbol{E}\boldsymbol{\xi}, \tag{28}$$

$$C_P = \boldsymbol{\xi}^{\mathrm{T}}\boldsymbol{P}\boldsymbol{\xi}, \tag{29}$$

$$C_T = \boldsymbol{\xi}^{\mathrm{T}}\boldsymbol{T}\boldsymbol{\xi}, \tag{30}$$

$$C_{T_s} = \boldsymbol{\xi}^{\mathrm{T}}\boldsymbol{K}\boldsymbol{\xi}, \tag{31}$$

where $(\,)^{\mathrm{T}}$ denotes the transpose of a matrix and $\boldsymbol{\xi}^{\mathrm{T}} = \{\xi_0, \xi_1, \xi_2\}$. $\boldsymbol{E}$, $\boldsymbol{P}$, $\boldsymbol{T}$ and $\boldsymbol{K}$, the matrices of the quadratic forms, are given in Wu (1971*b*).†

The optimum problem then is to minimize the quadratic form C_E subject to the constraint

$$C_T = C_{T,0} > 0. \tag{32}$$

Wu has pointed out that application of variational methods to this problem fails to yield the optimum because the quadratic form C_E is singular,‡ since one of the three eigenvalues of $\boldsymbol{E}$ is identically zero. The quadratic form C_E must first be reduced to a non-singular one of a lower order, which is then tractable by the usual variational methods. Wu's analysis shows that ξ_0 is a free parameter in the problem and hence the solution is non-unique. $\bar{C}_{T,0} = C_{T,0}/\xi_0^2$, termed the proportional loading parameter by Wu, is likewise a free parameter in the problem.

The normal modes of $\boldsymbol{E}$, in terms of which we will recast the solution, are given by (in normalized form)

$$\boldsymbol{\phi}_1 = [(4+k^2)(4+2k^2)]^{-\frac{1}{2}} \begin{Bmatrix} (4+k^2)(4+2k^2) \\ -k^2 \\ -2k \end{Bmatrix}, \tag{33}$$

† These are also obtained from the three-dimensional results of the preceding section after replacing c/A by c and setting the induced downwash $W_1 = 0$.

‡ C_P is indefinite in both two and three dimensions.

$$\boldsymbol{\Phi}_2 = (4+k^2)^{-\frac{1}{2}} \begin{Bmatrix} 0 \\ 2 \\ -k \end{Bmatrix} \tag{34}$$

$$\boldsymbol{\Phi}_3 = (4+2k^2)^{-\frac{1}{2}} \begin{Bmatrix} k \\ k \\ 2 \end{Bmatrix}, \tag{35}$$

where $k = \omega c/U$ is the reduced frequency. The first and third modes consist of combined pitch and heave motion, whereas the second mode represents pure pitching motion. The first mode has some interesting properties and plays a central role in the present optimum solution. We discuss its properties in some detail.

It can be shown that, for $\boldsymbol{\xi} = \boldsymbol{\Phi}_1$,

$$C_E = C_P = C_T = 0. \tag{36}$$

$\boldsymbol{\Phi}_1$ is, in fact, the same as the special set of values $\{\xi_0, \xi_1, \xi_2\}$ of Wu (1971*b*), who points out that this set corresponds to zero circulation around the airfoil, whereby no vorticity is shed in the wake. We refer to $\boldsymbol{\Phi}_1$ as the 'invisible mode', since it does not contribute to the average value of the energetic quantities and produces no wake vorticity. It must be noted, however, that, although the average thrust is zero, because of the unsteadiness of the airfoil motion, the leading-edge suction force and the thrust from the normal force are generally both non-zero ($\overline{T}_P = -\overline{T}_S \neq 0$). Furthermore, although the unsteady lift and moment are generally non-zero because of added mass effects, the average rate of work done by the airfoil $\overline{P}$ is zero.

Wu (1971*a*) has shown that for an oscillating airfoil $C_E \propto |b_0 + b_1|^2$ and $C_P \propto (b_0 + b_1)$, where b_n is defined in (4). It follows that the hydrodynamic efficiency of the invisible mode is 100 %. This is analogous to the Froude efficiency of a propeller, which tends to 100 % as the disk loading vanishes. However, since the invisible mode violates the conditions of fixed positive thrust (32), it, by itself, does not constitute the optimum.

As $k \to 0$, the invisible mode tends to perfect geometric feathering, where the airfoil pitching motion is such that the airfoil stays tangent to the path traversed in space by the heaving motion of the pitch axis. Analogously, in a time-averaged sense, the invisible mode can be thought of as perfect unsteady feathering, since it sheds no vorticity in the wake, requires the least amount of power to maintain the airfoil motion, and produces zero average thrust (or drag).

When the amplitude ratio and phase advance of pitch relative to heave, Z_P and α_P, and the hydrodynamic efficiency η for the invisible mode are plotted and superimposed on those for the optimum motion of the airfoil (Wu 1971*b*), they are found to form an upper envelope for the family of optimum solutions ($\bar{C}_{T,0}$ is the free parameter). With decreasing $\bar{C}_{T,0}$ and/or increasing reduced frequency k, all optimum solutions approach the invisible mode. The invisible mode thus plays a central role in the optimum solution. This is discussed formally in the next section.

3.1. *Recast form of the optimum solution*

In order to understand better the structure of the optimum and the role of the invisible mode in it, we recast the solution in terms of the normal modes of the energy-loss-rate matrix $\boldsymbol{E}$. Denoting the optimum solution by $\boldsymbol{\xi}^*$, we set

$$\boldsymbol{\xi}^* = \sum_{i=1}^{3} \gamma_i \boldsymbol{\Phi}_i, \tag{37}$$

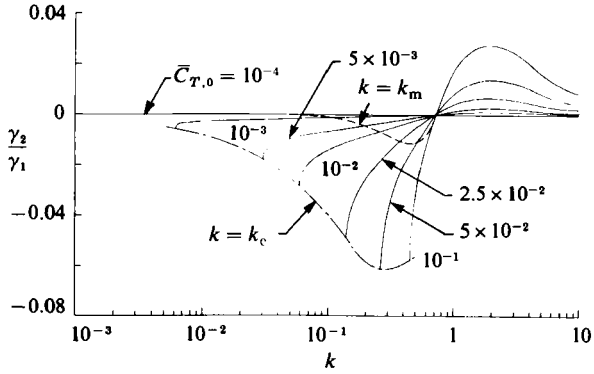

FIGURE 6. Amount of the second mode relative to the invisible mode for the optimum motion of an oscillating airfoil.

where the weighting functions γ_i indicate the amount of each of the modes present in $\boldsymbol{\xi}^*$. $\boldsymbol{\phi}_i$ are given in (33)–(35). To determine γ_i, we premultiply both sides of (37) by $\boldsymbol{\phi}_j^{\mathrm{T}}$ and use the orthogonality property $\boldsymbol{\phi}_j^{\mathrm{T}} \boldsymbol{\phi}_i = \delta_{ij}$ to obtain

$$\gamma_j = \boldsymbol{\phi}_j^{\mathrm{T}} \boldsymbol{\xi}^*, \quad j = 1, 2, 3, \tag{38}$$

where δ_{ij} is the Kronecker delta function.

The three equations in (38) determine only two of the three functions γ_1, γ_2, and γ_3 because, as mentioned earlier, ξ_0 is arbitrary. Thus, we find

$$\frac{\gamma_2}{\gamma_1} = \frac{\phi_{21} + \phi_{22}(\xi_1^*/\xi_0) + \phi_{23}(\xi_2^*/\xi_0)}{\phi_{11} + \phi_{12}(\xi_1^*/\xi_0) + \phi_{13}(\xi_2^*/\xi_0)}, \tag{39}$$

$$\frac{\gamma_3}{\gamma_1} = \frac{\phi_{31} + \phi_{32}(\xi_1^*/\xi_0) + \phi_{33}(\xi_2^*/\xi_0)}{\phi_{11} + \phi_{12}(\xi_1^*/\xi_0) + \phi_{13}(\xi_2^*/\xi_0)}, \tag{40}$$

and rewrite (37) as

$$\boldsymbol{\xi}^* = \gamma_1 \left[\boldsymbol{\phi}_1 + \left(\frac{\gamma_2}{\gamma_1}\right) \boldsymbol{\phi}_2 + \left(\frac{\gamma_3}{\gamma_1}\right) \boldsymbol{\phi}_3 \right], \tag{41}$$

where we have chosen the amount of the invisible mode γ_1 to be the free parameter rather than ξ_0. The reason for this choice will become clear later. Accordingly, we replace the proportional loading parameter $\bar{C}_{T,0}$ with a modified loading parameter $\tilde{C}_{T,0} = C_{T,0}/\gamma_1^2$ which is related to the former through

$$\tilde{C}_{T,0} = \bar{C}_{T,0} \left[\phi_{11} + \left(\frac{\gamma_2}{\gamma_1}\right) \phi_{21} + \left(\frac{\gamma_3}{\gamma_1}\right) \phi_{31} \right]^2. \tag{42}$$

The amounts of the second and third modes, relative to the invisible mode, present in the solution, are shown in figures 6 and 7. The lines denoted by $k = k_c$ and $k = k_m$ represent, respectively, the value of k below which no optimum exists and the value of k for which the fraction of thrust contributed by the leading-edge suction force is a minimum. Herein, we refer to the optimum for $k = k_m$ as 'superoptimum,' since in reality large leading-edge suction force is generally associated with leading-edge stall.

In figures 6 and 7, it is seen that, in general, with decreasing $\bar{C}_{T,0}$ and/or increasing k, both γ_2/γ_1 and γ_3/γ_1 decrease and the invisible mode increasingly dominates the solution. Figure 8 depicts $\tilde{C}_{T,0}$ as a function of k and $\bar{C}_{T,0}$. We note

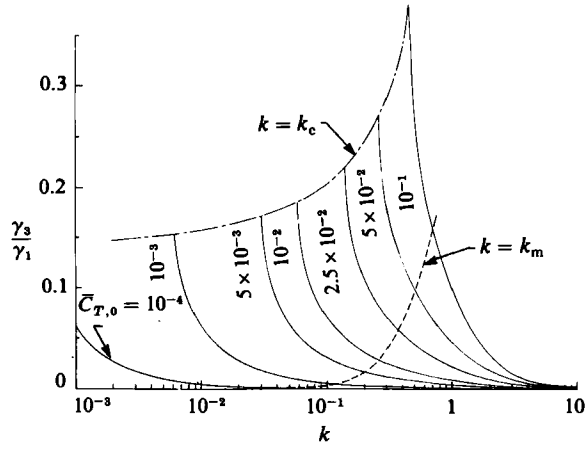

FIGURE 7. Amount of the third mode relative to the invisible mode for the optimum motion of an oscillating airfoil.

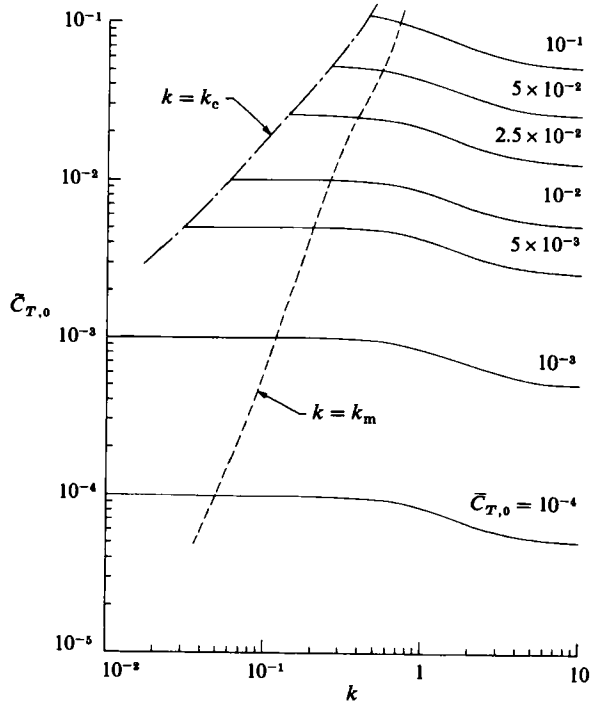

FIGURE 8. $\bar{C}_{T,0}$ as a function of k and $\bar{C}_{T,0}$ for the optimum motion of an oscillating airfoil.

that, for small values of $\bar{C}_{T,0}$ and k, $\bar{C}_{T,0} \approx \bar{C}_{T,0}$. This is because, under these conditions, the solution is dominated by the invisible mode, which tends to pure heave as $k \to 0$ (see (33)).

Thus the optimum consists primarily of the invisible mode with a small amount of the third mode (of the order of 10%) and an even smaller amount of the second mode (of the order of 1%). The invisible mode is responsible for the high η achieved by the optimum, whereas the other modes are necessary to attain the

prescribed level of thrust. The superoptimum achieves higher η at lower values of $\bar{C}_{T,0}$. From the recast form of the optimum, it becomes clear that the reason for the non-uniqueness of the present solution is the invisible mode, an arbitrary amount of which (γ_1) is present in the solution.

Strictly speaking, the recast results should be presented with $\tilde{C}_{T,0}$ as a parameter rather than $\bar{C}_{T,0}$. However, since there is a one-to-one correspondence between ξ_0 and γ_1 (see (41)) and hence also between $\bar{C}_{T,0}$ and $\tilde{C}_{T,0}$ (see figure 8), the above presentation is adequate.

4. Optimum motion of an oscillating wing

In this section, we use the three-dimensional energetic quantities of §2 to determine the optimum motion of a high-aspect-ratio wing oscillating harmonically in combined pitch and heave (see figure 1). The wing motion is described by (1). The use of lifting-line theory restricts the analysis to wings of large aspect ratio and slender planform oscillating at relatively low reduced frequencies.

In matrix notation, we represent the average total energetic quantities for the finite wing as

$$C_{\mathscr{E}} = \boldsymbol{\xi}^{\mathrm{T}} \boldsymbol{\mathscr{E}} \boldsymbol{\xi}, \tag{43}$$

$$C_{\mathscr{P}} = \boldsymbol{\xi}^{\mathrm{T}} \boldsymbol{\mathscr{P}} \boldsymbol{\xi}, \tag{44}$$

$$C_{\mathscr{T}} = \boldsymbol{\xi}^{\mathrm{T}} \boldsymbol{\mathscr{T}} \boldsymbol{\xi}, \tag{45}$$

$$C_{\mathscr{T}_{\mathrm{s}}} = \boldsymbol{\xi}^{\mathrm{T}} \boldsymbol{\mathscr{K}} \boldsymbol{\xi}, \tag{46}$$

where $\boldsymbol{\mathscr{E}}$, $\boldsymbol{\mathscr{P}}$, $\boldsymbol{\mathscr{T}}$, and $\boldsymbol{\mathscr{K}}$ are the respective matrices of the quadratic forms for (average) total energy-loss rate, total required power, total thrust, and total leading-edge suction force. They are symmetric by construction and have the additional properties $Q_{22} = Q_{33}$ and $Q_{23} = 0$, where Q_{ij} is the matrix element (i, j).

Here, as in two dimensions, the quadratic form $C_{\mathscr{P}}$ is indefinite and it is crucial first to identify what type of quadratic form $C_{\mathscr{E}}$ is. To this end we temporarily adopt the strip-theory viewpoint and investigate the possibility of distributing two-dimensional invisible modes across the span. It can be shown that the invisible mode at spanwise station y is given by

$$\frac{\xi_1}{\xi_0} = \frac{-k_0 k}{4+k^2}, \quad \frac{\xi_2}{\xi_0} = \frac{-2k_0}{4+k^2}. \tag{47}$$

Here, the right-hand sides are functions of y because $k = \omega c(y)/(UA)$, but the left-hand sides are independent of y, since the wing is rigid. Therefore (47) can be enforced at one or, at most, a finite number of stations y, depending on the planform shape, but not at all y.† Wherever (47) is violated, spanwise vorticity is shed, and the circulation is non-zero and varies with y, which gives rise to trailing vorticity. Including the three-dimensional effects modifies this picture slightly, but, since the corrections are of higher order, the basic picture remains the same. This means that no non-trivial unsteady motion of a rigid wing exists that does not produce a wake of vorticity. In other words, no invisible mode for the rigid wing of finite span exists and $C_{\mathscr{E}}$ is positive definite.

The three-dimensional optimum may be stated as: minimize the quadratic form $C_{\mathscr{E}}$ subject to

$$C_{\mathscr{T}} = C_{\mathscr{T},0} > 0. \tag{48}$$

† We exclude the rectangular planform from consideration, because of blunt wingtips.

As in two dimensions, this is equivalent to minimizing a new function $C'_{\mathscr{E}} = C_{\mathscr{E}} - \lambda C_{\mathscr{P}}$ subject to the same condition, λ being a Lagrange multiplier. Denoting the elements of $\mathscr{E}$ and $\mathscr{P}$ by E_{ij} and P_{ij} respectively, we have

$$C_{\mathscr{E}} = E_{11}\xi_0^2 + E_{22}(\xi_1^2+\xi_2^2) + 2E_{12}\xi_0\xi_1 + 2E_{13}\xi_0\xi_2, \tag{49}$$

$$C_{\mathscr{P}} = P_{11}\xi_0^2 + P_{22}(\xi_1^2+\xi_2^2) + 2P_{12}\xi_0\xi_1 + 2P_{13}\xi_0\xi_2. \tag{50}$$

Since $C_{\mathscr{E}}$ is positive definite, the optimum is obtained by the use of the usual variational methods. Thus we set

$$\frac{\partial}{\partial\xi_i}(C_{\mathscr{E}} - \lambda C_{\mathscr{P}}) = 0, \quad i = 0, 1, 2, \tag{51}$$

$$C_{\mathscr{T}} = C_{\mathscr{P}} - C_{\mathscr{E}} = C_{\mathscr{T},0} > 0. \tag{52}$$

λ is the solution of the cubic secular equation

$$|\mathscr{E} - \lambda\mathscr{P}| = 0 \tag{53}$$

or
$$(E_{22}-\lambda P_{22})[(E_{11}-\lambda P_{11})(E_{22}-\lambda P_{22}) - (E_{12}-\lambda P_{12})^2 - (E_{13}-\lambda P_{13})^2] = 0. \tag{54}$$

The root $\lambda_3 = E_{22}/P_{22}$ corresponds to pure pitching motion, which is not the optimum. The remaining roots, λ_1 and λ_2, are the solutions of the quadratic equation

$$a\lambda^2 + b\lambda + c = 0, \tag{55}$$

where
$$\left.\begin{aligned} a &= P_{11}P_{22} - P_{12}^2 - P_{13}^2, \\ b &= 2E_{12}P_{12} + 2E_{13}P_{13} - E_{11}P_{22} - E_{22}P_{11}, \\ c &= E_{11}E_{22} - E_{12}^2 - \mathrm{E}_{13}^2. \end{aligned}\right\} \tag{56}$$

λ_1 and λ_2 would be real, as required for physically meaningful solutions, if $b^2 - 4ac \geqslant 0$.

Substituting λ in (51), we obtain

$$\frac{\xi_1}{\xi_0} = -\frac{E_{12}-\lambda P_{12}}{E_{22}-\lambda P_{22}}, \tag{57}$$

$$\frac{\xi_2}{\xi_0} = -\frac{E_{13}-\lambda P_{13}}{E_{22}-\lambda P_{22}}. \tag{58}$$

The hydrodynamic efficiency is given by

$$\eta = 1 - \frac{E_{11} + E_{22}[(\xi_1/\xi_0)^2 + (\xi_2/\xi_0)^2] + 2E_{12}(\xi_1/\xi_0) + 2E_{13}(\xi_2/\xi_0)}{P_{11} + P_{22}[(\xi_1/\xi_0)^2 + (\xi_2/\xi_0)^2] + 2P_{12}(\xi_1/\xi_0) + 2P_{13}(\xi_2/\xi_0)}. \tag{59}$$

The λ corresponding to the larger η ($0 \leqslant \eta \leqslant 1$) is the optimum. ξ_0 is then obtained from the condition (52):

$$\xi_0^2 = C_{\mathscr{T},0}\left\{(P_{11}-E_{11}) + (P_{22}-E_{22})\left[\left(\frac{\xi_1}{\xi_0}\right)^2 + \left(\frac{\xi_2}{\xi_0}\right)^2\right] + 2(P_{12}-E_{12})\left(\frac{\xi_1}{\xi_0}\right) + 2(P_{13}-E_{13})\left(\frac{\xi_2}{\xi_0}\right)\right\}^{-1}. \tag{60}$$

In analogy with the two-dimensional optimum, we may rewrite this as an expression for the proportional loading parameter $\bar{C}_{\mathscr{T},0} = C_{\mathscr{T},0}/\xi_0^2$. It is important to note that, in contrast with the two-dimensional case, the present optimum solution is unique

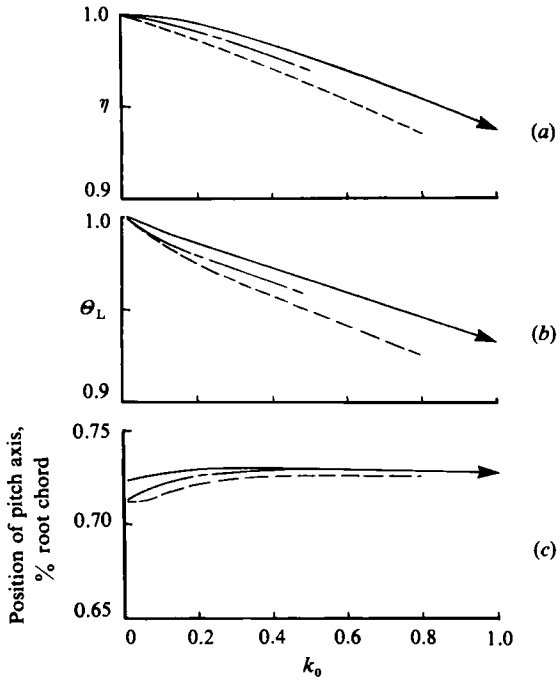

FIGURE 9. Hydrodynamic efficiency, proportional loading parameter and location of pitch axis for the optimum motion of an oscillating elliptic wing; ——, ST; —·—, $A = 16$; – – –, $A = 8$.

(at least for low reduced frequencies). This is a direct result of $C_{\mathscr{E}}$ being positive definite.

The amplitude ratio and the phase advance of pitch relative to heave are obtained from (21). The fraction of thrust coming from the leading-edge suction force is given by

$$\frac{C_{\mathscr{T}_S}}{C_{\mathscr{T}}} = (\bar{C}_{\mathscr{T},0})^{-1}\left\{K_{11}+K_{22}\left[\left(\frac{\xi_1}{\xi_0}\right)^2+\left(\frac{\xi_2}{\xi_0}\right)^2\right]+2K_{12}\left(\frac{\xi_1}{\xi_0}\right)+2K_{13}\left(\frac{\xi_2}{\xi_0}\right)\right\}, \tag{61}$$

where K_{ij} denotes the elements of $\mathscr{K}$ (see (46)). To understand the optimum better, it is helpful to express the solution in terms of Lighthill's (1970) alternative description, (19).

Results for the optimum are obtained from the three-dimensional energetic quantities of §2 and the above analysis. Figures 9–11 show the optimum motion for an elliptic wing. Calculations are carried out for $0 \leqslant k_0 \leqslant 1$ and $A = 8$ and 16. Strip-theory calculations ($W_I = 0$) are also shown for comparison. For each aspect ratio, the results are cut off at the value of k_0 corresponding to the approximate range of applicability of the lifting-line theory at that A (see figure 18 of Ahmadi & Widnall 1982). It is seen that, with increasing A, the three-dimensional results approach the corresponding strip-theory values as expected. Figure 9(*a*) shows that the highest η is achieved by the strip-theory case. This is due to the absence of induced downwash, which normally increases $C_{\mathscr{E}}$, decreases $C_{\mathscr{P}}$, and hence reduces $\eta = 1 - C_{\mathscr{E}}/C_{\mathscr{P}}$, as pointed out earlier.

Figures 9(*b*) and (*c*) show the optimum motion in terms of Lighthill's parameters. We note that the optimum position of the pitch axis is at about 73 % root chord and

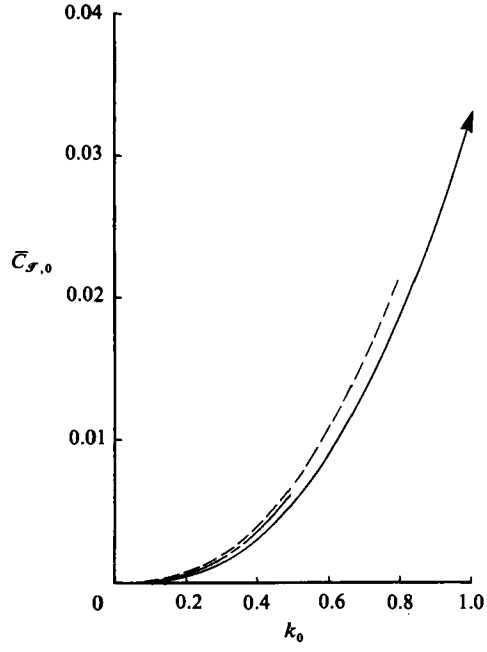

FIGURE 10. Proportional loading parameter for the optimum motion of an oscillating elliptic wing; ——, ST; —·—, $A = 16$; — — —, $A = 8$.

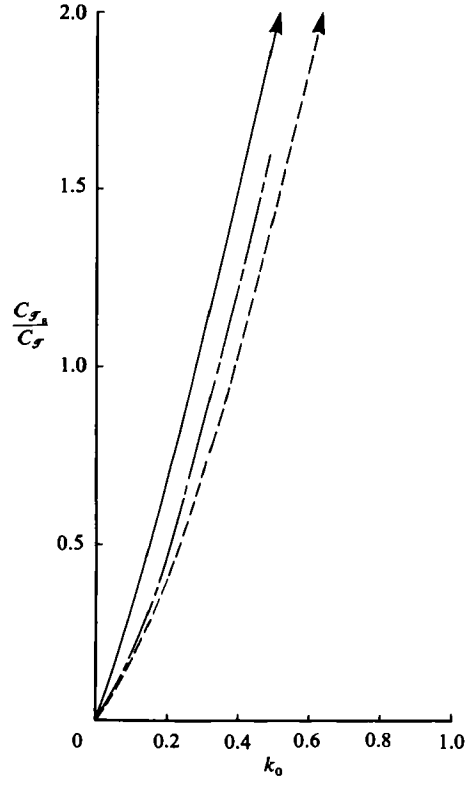

FIGURE 11. Ratio of leading-edge suction force to thrust for the optimum motion of an oscillating elliptic wing; ——, ST; —·—, $A = 16$; — — —, $A = 8$.

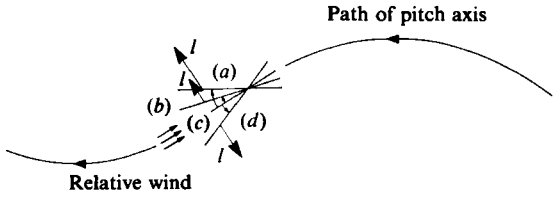

FIGURE 12. Sinusoidal motion of a flat-plate airfoil under quasi-steady condition, (*a*) $\theta_L = 0$, pure heave, $\bar{T} > 0$; (*b*) $0 < \theta_L < 1$, $\bar{T} > 0$; (*c*) $\theta_L = 1$, perfect geometric feathering, $\bar{T} = 0$; (*d*) $\theta_L > 1$, $\bar{T} < 0$.

remains fairly constant with increasing k_0. In relation to θ_L, we recall that $\theta_L = 0$ and $\theta_L = 1$ represent pure heave and perfect geometric feathering, respectively. To understand better the behaviour of θ_L for the optimum, we first consider the two-dimensional quasi-steady case, where for positive average thrust $0 \leqslant \theta_L < 1$; for zero average thrust $\theta_L = 1$; and for negative average thrust $\theta_L > 1$. These ideas are depicted schematically in figure 12. We recall that, in quasi-steady flow, thrust is just the horizontal component of lift.

In three dimensions, the induced downwash normally reduces the effective incidence of wing sections, thereby reducing the thrust. In order to restore the thrust, we increase the effective incidence of the wing by lowering θ_L further below unity. This, on the one hand, represents a greater angular deviation of the wing from geometric feathering in the direction of positive thrust ($0 \leqslant \theta_L < 1$), and, on the other, is a reduction in pitch amplitude (measured from the horizontal). We see the same trend in figure 9(*b*), where θ_L for cases of finite span are farther below unity than the strip-theory values. Presumably, the same trend holds at higher k_0 (as seen in figure 9*b*) where the problem is more complex owing to unsteady effects.

Figure 10 shows that, with decreasing aspect ratio, the proportional loading parameter increases. Since $C_{\mathcal{T},0}$ is prescribed, figure 10 is to be interpreted as giving ξ_0 (non-dimensional heave amplitude), which decreases with decreasing A and/or increasing k_0. It is thus seen that, with decreasing A, both pitch and heave amplitudes are reduced. Furthermore, the behaviour of θ_L in figure 9(*b*) indicates that the amplitude of pitch is reduced more than that of heave (non-dimensional).

From the above considerations, the three-dimensional optimum can be described as follows. Compared with the strip-theory case, the wing of finite span oscillates with smaller heave amplitude because, for fixed k_0, the larger the heave amplitude, the stronger the trailing and shed vorticity and unsteady induced downwash, tending to reduce η. With the smaller heave amplitude, the question is raised as to how the wing maintains the prescribed level of thrust. The answer lies in the pitch amplitude, which, measured from the position of perfect geometric feathering ($\theta_L = 1$), is increased in the direction of increasing thrust ($\theta_L < 1$).

Figure 11 shows that the fraction of thrust from the leading-edge suction force decreases with decreasing A because induced downwash increases, reducing the suction force. In contrast to the two-dimensional optimum, in three dimensions there is no superoptimum (except for a trivial solution at $k_0 = 0$). Figure 11 shows that the range of k_0 where $C_{\mathcal{T}_s}/C_{\mathcal{T}}$ is acceptably small (to avoid leading-edge stall) is not very large. For example for $(C_{\mathcal{T}_s}/C_{\mathcal{T}}) < 40\,\%$, $k_0 \lesssim 0.2$, which is a somewhat small range. Leading-edge sweepback reduces $C_{\mathcal{T}_s}/C_{\mathcal{T}}$ and thus increases the range of k_0 for which $C_{\mathcal{T}_s}/C_{\mathcal{T}}$ is acceptably small (see Chopra & Kambe 1977).

In summary, we have the following differences between the two- and three-dimensional optimum solutions. The three-dimensional optimum is unique while the two-dimensional one is non-unique. The numerical examples considered show no k_c and k_m for the three-dimensional optimum. Hence, in contrast with the two-dimensional case, in three dimensions there is no superoptimum and the solution seems to exist for all reduced frequencies (at least for low reduced frequencies). The above differences also make questionable Wu's (1971*b*) strip-theory application of the two-dimensional optimum to a three-dimensional wing.

We end this section with some comments on the optimum-shape problem for a flexible wing. In particular, we consider the semi-flexible wing defined by

$$h(x,y,t) = \left\{\frac{1}{2}\left(\frac{c_0}{A}\right)\xi_0(y) + [\xi_1(y) + \mathrm{j}\xi_2(y)]\,x\right\} e^{\mathrm{j}\omega t} \quad \left(|x| \leqslant \frac{c(y)}{A},\ |y| \leqslant b\right). \tag{62}$$

Here, it is best to assume a number of suitably chosen spanwise modes for each of $\xi_0(y)$, $\xi_1(y)$, and $\xi_2(y)$. The unsteady lifting-line theory can then be used to calculate the energetic quantities needed for optimization, as in §2. Here, $C_{\mathscr{P}}$ is indefinite. To determine the type of the quadratic form $C_{\mathscr{E}}$, we again temporarily adopt the strip-theory viewpoint and investigate the possibility of distributing two-dimensional invisible modes across the span.

It can be shown that the invisible mode at spanwise station y is given by

$$\frac{\xi_1(y)}{\xi_0(y)} = \frac{-k_0 k}{4+k^2}, \quad \frac{\xi_2(y)}{\xi_0(y)} = \frac{-2k_0}{4+k^2}. \tag{63}$$

Since, for the semi-flexible wing, $\xi_0(y)$, $\xi_1(y)$ and $\xi_2(y)$ are arbitrary functions of y, (63) can be maintained at every spanwise station y. Then, sectional thrust and power required as well as the circulation $\Gamma(y,t)$ will be identically zero across the span. Hence, no spanwise or streamwise vorticity will be shed from the wing. This means that, for the semi-flexible wing described by (62), there exists a non-trivial unsteady motion defined by (63), for which $C_{\mathscr{E}} = C_{\mathscr{P}} = C_{\mathscr{T}} = 0$ and $\Gamma(y,t) = 0$. That is, there exists an invisible mode, and $C_{\mathscr{E}}$ is positive semi-definite. Therefore, the optimization requires that the singular quadratic form $C_{\mathscr{E}}$ first be reduced to a non-singular one of a lower order which can be handled by the usual variational methods. The resulting optimum solution will be non-unique.

This work was sponsored in part by NASA Grant NGR 22-009-818. This support is gratefully acknowledged. The first author is also grateful to his former employer Bolt Beranek and Newman Inc. for providing support during and for the preparation of this paper.

Appendix

This appendix summarizes the principal results of the unsteady lifting-line theory used in this paper (Ahmadi 1980; Ahmadi & Widnall 1982, 1985). The theory treats a spanwise flexible unswept wing of large aspect ratio oscillating at low reduced frequency in inviscid incompressible flow. The linearized theory is formulated in terms of the acceleration potential $\psi(x,t) = [p_\infty - p(x,t)]/\rho$ and solved by the method of matched asymptotic expansions, which reduces the problem from a singular integral equation to quadrature. For prescribed wing shapes and motions, the theory yields

the complete pressure field, airloads (chordwise and spanwise pressure distributions) and unsteady induced downwash in closed form.

The theory is developed for a wing whose planform shape is given by $x = \pm c(y)/A$, $|y| \leqslant b$, $z = 0$, and whose transverse displacements are described by (see figure 1)

$$z = h(x,y,t) = \left[\frac{h_0(y)}{A} + \alpha(y)\,x\right] e^{j\omega t}$$
$$= \left\{\frac{1}{2}\left(\frac{c_0}{A}\right)\xi_0(y) + [\xi_1(y) + j\xi_2(y)]\,x\right\} e^{j\omega t} \quad \left(|x| \leqslant \frac{c(y)}{A},\ |y| \leqslant b\right). \tag{A 1}$$

The theory shows that finite-span effects arise from unsteady induced downwash W_I, which is shown to be a convecting sinusoidal gust

$$W_I(x,y,t) = \tilde{W}_g(y)\, e^{-j\bar{\omega}x}\, e^{j\omega t} \quad \left(|x| \leqslant \frac{c(y)}{A},\ |y| \leqslant b\right), \tag{A 2}$$

whose complex amplitude $\tilde{W}_g(y)$ is given by

$$\tilde{W}_g(y) = \frac{1}{4\pi\rho U}\left\{\text{⨍}_{-b}^{b} \frac{\tilde{l}_{2D}(\eta)}{(y-\eta)^2}\Sigma(\bar{\omega}\,|y-\eta|)\,d\eta - j\bar{\omega}\int_{-b}^{b}\frac{\tilde{l}_{2D}(\eta)-\tilde{l}_{2D}(y)}{|y-\eta|}d\eta\right.$$
$$\left. + 2j\bar{\omega}\,\tilde{l}_{2D}(y)\left\{1-\gamma-j\tfrac{1}{2}\pi-\log\mu_0-\tfrac{1}{2}\log 4\left[1-\left(\frac{y}{b}\right)^2\right]\right\}\right\}, \tag{A 3}$$

where $\tilde{l}_{2D}(y)$ is the two-dimensional unsteady section lift (see below); $\bar{\omega} = \omega/U$; $\gamma = 0.577\ldots$ is the Euler constant; $\mu_0 = \bar{\omega}b$ is the reduced frequency based on the semi-span; ⨍ denotes the principal value of an integral in the sense of Hadamard (see Mangler 1951); and $\Sigma(\eta)$ is the kernel function of unsteady lifting-line theory:

$$\Sigma(\mu) = \mu\{K_1(\mu) + j\tfrac{1}{2}\pi[I_1(\mu) - L_1(\mu)]\}. \tag{A 4}$$

I_1, K_1, and L_1 are, respectively, modified Bessel functions of the first and second kind of order one and modified Struve function of order one.

Interaction of this induced sinusoidal gust with wing sections modifies the local two-dimensional pressure field ψ_{2D} by an amount equal to the pressure field of the interaction of a convecting sinusoidal gust with an airfoil ψ_{Sears}, i.e. the Sears problem (Sears 1941). The pressure field of the wing is given by

$$\tilde{\psi}(\boldsymbol{x}) = \tilde{\psi}_{2D}(\hat{\boldsymbol{x}}) + \tilde{\psi}_{Sears}(\hat{\boldsymbol{x}}) - \frac{1}{4\pi\rho}\frac{\partial}{\partial z}\int_{-b}^{b}\frac{\tilde{l}_{2D}(\eta)}{[x^2+(y-\eta)^2+z^2]^{\frac{1}{2}}}d\eta + \frac{1}{2\pi\rho}\tilde{l}_{2D}(y)\frac{z}{x^2+z^2}, \tag{A 5}$$

where (ˆ) denotes variables magnified by the aspect ratio. These are appropriate in the 'inner region', i.e. distances from the wing of the order of chord $c(y)/A$, as $A \to \infty$ (see Ahmadi 1980).

In the neighbourhood of the wing, the last two terms on the right of (A 5) cancel and the wing-pressure distribution $\Delta\tilde{p}(x,y) = \tilde{\psi}(\hat{x},y,0+) - \tilde{\psi}(\hat{x},y,0-)$ is given by the sum of $\tilde{\psi}_{2D}(\hat{\boldsymbol{x}})$ and $\tilde{\psi}_{Sears}(\hat{\boldsymbol{x}})$, both of which are obtained from the unsteady airfoil theory of Wu (1971*a*). They are given by

$$\tilde{\psi}_{2D}(\hat{\boldsymbol{x}}) = \mathrm{IP}_i\left\{B_1(y)\left[-\hat{\zeta}^2 + \left(\hat{\zeta}^2 + c\hat{\zeta} + \frac{c^2}{2}\right)\lambda\right] + B_2(y)\,[-\hat{\zeta} + (\hat{\zeta}^2 - c^2)^{\frac{1}{2}}] + B_3(y)\,[\lambda - 1]\right\}, \tag{A 6}$$

where IP_i denotes the imaginary part of a complex quantity with respect to the spatial complex variable i,

$$\left.\begin{aligned} \lambda &= \left[\frac{\xi - c}{\xi + c}\right]^{\frac{1}{2}}, \\ B_1(y) &= \frac{1}{2c^2} U^2 k^2 \alpha, \\ B_2(y) &= \frac{1}{c} U^2 \left[k_0 k \frac{h_0}{c_0} - 2\mathrm{j}k\alpha\right], \\ B_3(y) &= U^2 \left\{-\tfrac{1}{4}(k^2 - 2\mathrm{j}k)\alpha - \left[\mathrm{j}k_0 \frac{h_0}{c_0} + (1 + \tfrac{1}{2}\mathrm{j}k)\alpha\right] C(k)\right\} \end{aligned}\right\} \quad \text{(A 7)}$$

and

$$\tilde{\psi}_{\text{Sears}}(\hat{x}) = \mathrm{IP}_1\{U \tilde{W}_g(y)\, S(k)\,[\lambda - 1]\}, \quad \text{(A 8)}$$

where $k = \bar{\omega} c(y)/A$ is the reduced frequency based on the local semi-chord. $S(k)$ is the Sears function (Sears 1941):

$$S(k) = \mathrm{j}J_1(k) + [J_0(k) - \mathrm{j}J_1(k)]\, C(k). \quad \text{(A 9)}$$

$C(k)$ is Theodorsen's function (Theodorsen 1935):

$$\begin{aligned} C(k) &= \frac{H_1^{(2)}(k)}{H_1^{(2)}(k) + \mathrm{j}H_0^{(2)}(k)} \\ &= \frac{J_1(J_1 + Y_0) + Y_1(Y_1 - J_0)}{(J_1 + Y_0)^2 + (Y_1 - J_0)^2} + \mathrm{j}\frac{-(Y_1 Y_0 + J_1 J_0)}{(J_1 + Y_0)^2 + (Y_1 - J_0)^2}, \end{aligned} \quad \text{(A 10)}$$

where $H_n^{(2)}(z) = J_n(z) - \mathrm{j}\, Y_n(z)$ is the Hankel function of the second kind of order n, and Y_n are respectively Bessel functions of the first and second kind of order n.

Similarly, section lift and moment are given by

$$\tilde{l}(y) = \tilde{l}_{2\mathrm{D}}(y) + \tilde{l}_{\text{Sears}}(y), \quad \tilde{m}(y) = \tilde{m}_{2\mathrm{D}}(y) + \tilde{m}_{\text{Sears}}(y), \quad \text{(A 11)}$$

where

$$\left.\begin{aligned} \tilde{l}_{2\mathrm{D}}(y) &= \pi\rho U^2 \left(\frac{c}{A}\right)\left\{\mathrm{j}k\alpha - k_0 k\left(\frac{h_0}{c_0}\right) + \left[(2 + \mathrm{j}k)\alpha + 2\mathrm{j}k_0\left(\frac{h_0}{c_0}\right)\right] C(k)\right\}, \\ \tilde{m}_{2\mathrm{D}}(y) &= \frac{\pi}{2}\rho U^2 \left(\frac{c}{A}\right)^2 \left\{(\mathrm{j}k - \tfrac{1}{4}k^2)\alpha - \left[(2 + \mathrm{j}k)\alpha + 2\mathrm{j}k_0\left(\frac{h_0}{c_0}\right)\right] C(k)\right\} \end{aligned}\right\} \quad \text{(A 12)}$$

are the familiar two-dimensional unsteady lift and moment for an airfoil in combined pitch and heave, and

$$\tilde{l}_{\text{Sears}}(y) = 2\pi\rho U^2 \left(\frac{c}{A}\right)\frac{\tilde{W}_g(y)}{U} S(k), \quad \tilde{m}_{\text{Sears}}(y) = \pi\rho U^2 \left(\frac{c}{A}\right)^2 \frac{\tilde{W}_g(y)}{U} S(k) \quad \text{(A 13)}$$

are the corresponding three-dimensional corrections (lift and moment of the Sears problem).

Lifting-line theory requires the wing planform shape, i.e. $c(y)$, to vary slowly in the direction of the span. Blunt wingtips (e.g. rectangular planform) are thus excluded. They require additional local analysis near the tip. However, for elliptic and more-slender tip geometries, the theory yields convergent results.

Further details of the lifting-line theory and numerical schemes for calculating the finite-span effects are found in Ahmadi (1980).

REFERENCES

AHMADI, A. R. 1980 An asymptotic unsteady lifting-line theory with energetics and optimum motion of thrust-producing lifting surfaces. Ph.D. thesis, M.I.T., also as *NASA CR*-165679, 1981.

AHMADI, A. R. & WIDNALL, S. E. 1982 Unsteady lifting-line theory with applications. *AIAA Paper No.* 82-0354, presented at AIAA 20th Aerospace Sciences Conference, Orlando, FL.

AHMADI, A. R. & WIDNALL, S. E. 1985 Unsteady lifting-line theory as a singular perturbation problem. *J. Fluid Mech.* **153**, 59–81.

ARCHER, R. D., SAPUPPO, J. & BETTERIDGE, D. S. 1979 Propulsive characteristics of flapping wings. *Aero. J.* 355–371.

BENNET, A. G. 1970 A preliminary study of ornithopter aerodynamics. Ph.D. thesis, University of Illinois, Urbana.

BETTERIDGE, D. S. & ARCHER, R. D. 1974 A study of the mechanics of flapping wings. *Aer. Quart.*

CHOPRA, M. G. 1974 Hydrodynamics of lunate-tail swimming propulsion. *J. Fluid Mech.* **64**, 375–391.

CHOPRA, M. G. 1976 Large amplitude lunate-tail theory of fish locomotion. *J. Fluid. Mech.* **74**, 161–182.

CHOPRA, M. G. & KAMBE, T. 1977 Hydrodynamics of lunate-tail swimming propulsion. Part 2. *J. Fluid Mech.* **79**, 49–69.

GARRICK, I. E. 1936 Propulsion of a flapping and oscillating airfoil. *NACA Rep. No.* 567.

LAN, C. E. 1979 The unsteady quasi-vortex-lattice method with applications to animal propulsion. *J. Fluid Mech.* **93**, 747–765.

LIGHTHILL, M. J. 1970 Aquatic animal propulsion of high hydrodynamic efficiency. *J. Fluid Mech.* **44**, 265–301.

MANGLER, K. W. 1951 Improper integrals in theoretical aerodynamics. *ARC R&M* 2424.

REISSNER, E. 1947 Effect of finite span on the airload distributions for oscillating wings, I – Aerodynamic theory of oscillating wings of finite span. *NACA TN No.* 1194.

SEARS, W. R. 1941 Some aspects of non-stationary airfoil theory and its practical application. *J. Aero. Sci.* **8**, 104–108.

SIEKMANN, J. 1962 Theoretical studies of sea animal locomotion, part I. *Ing. Arch.* **31**, 214–228.

SIEKMANN, J. 1963 Theoretical studies of sea animal locomotion, part II. *Ing. Arch.* **32**, 40–50.

THEODORSEN, T. 1935 General theory of aerodynamic instability and the mechanism of flutter. *NACA TR*-496.

VON KÁRMÁN, T. & BURGERS, J. M. 1935 General aerodynamic theory – perfect fluids. In *Aerodynamic Theory* (ed. W. F. Durand), pp. 301–310. Julius Springer.

WAGNER, S. 1969 On the singularity method of subsonic lifting-surface theory. *J. Aircraft* **6**, 549–558.

WU, T. Y. 1961 Swimming of a waving plate. *J. Fluid Mech.* **10**, 321–344.

WU, T. Y. 1971*a* Hydrodynamics of swimming propulsion. Part 1. Swimming of a two-dimensional flexible plate at variable foward speed in an inviscid fluid. *J. Fluid Mech.* **46**, 337–355.

WU, T. Y. 1971*b* Hydrodynamics of swimming propulsion. Part 2. Some optimum shape problems. *J. Fluid Mech.* **46**, 521–544.